Oligonucleotide analogues with locked-amide linkages have therapeutic potential

Ysobel Baker
University of Oxford https://orcid.org/0000-0002-0266-771X
Cameron Thorpe
https://orcid.org/0000-0002-1980-678X
Jinfeng Chen
University of Oxford
Laura Poller
University of Oxford
Lina Cox
University of Oxford https://orcid.org/0000-0001-9450-6819
Pawan Kumar
University of Oxford
Wooi Fang Lim
University of Oxford https://orcid.org/0000-0002-1238-3040
Lillian Lie
University of Oxford
Graham McClorey
University of Oxford
Sven Epple
University of Oxford https://orcid.org/0000-0002-9078-3250
Daniel Singleton
ATDBio
Michael McDonough
University of Oxford https://orcid.org/0000-0003-4664-6942
Jack Hardwick
University of Oxford https://orcid.org/0000-0002-3117-1035
Kirsten Christensen
University of Oxford https://orcid.org/0000-0003-1683-2066
Matthew Wood
University of Oxford https://orcid.org/0000-0002-5436-6011
James Hall
University of Reading https://orcid.org/0000-0003-3716-4378
Afaf El-Sagheer

University of Oxford https://orcid.org/0000-0001-8706-1292
Tom Brown (tom.brown@chem.ox.ac.uk)
University of Oxford https://orcid.org/0000-0002-6538-3036

Article

Keywords:

Posted Date: May 4th, 2022

DOI: https://doi.org/10.21203/rs.3.rs-1542733/v1

Version of Record: A version of this preprint was published at Nature Communications on July 12th, 2022. See the published version at https://doi.org/10.1038/s41467-022-31636-2.

Abstract

Oligonucleotides that target mRNA have great promise as therapeutic agents for life-threatening conditions but suffer from poor bioavailability, hence high cost. As currently untreatable diseases come within the reach of oligonucleotide therapies, new analogues are urgently needed to address this. With this in mind we have developed reduced-charge oligonucleotides containing artificial LNA-amide linkages with improved gymnotic cell uptake, RNA affinity, stability and potency. To construct such oligonucleotides, five LNA-amide monomers (A, T, C, 5mC and G), where the 3´-OH is replaced by an ethanoic acid group, were synthesised in good yield and used in solid-phase oligonucleotide synthesis to form amide linkages with high efficiency. The artificial backbone causes minimal structural deviation to the DNA:RNA duplex. These studies indicate that splice-switching oligonucleotides containing LNA-amide linkages and phosphorothioates display improved activity relative to oligonucleotides lacking amides, highlighting the therapeutic potential of this technology.

Introduction

Antisense oligonucleotides (ASOs) are synthetic nucleic acid analogues that bind to RNA to regulate gene expression and interfere with protein synthesis[1, 2]. Their modes of action include steric blocking of translation[3], recruitment of RNase-H for degradation of mRNA[4], modulation of pre-mRNA splicing[5-7] and siRNA mediated gene silencing[8]. Therapeutic oligonucleotides in general have shown great promise as precision medicines, and have the potential to cure cancers, genetic disorders, and infectious diseases. They are particularly attractive because there are far more RNA targets than conventional protein targets in currently undruggable diseases[9]. Other advantages include their simple design criteria based on Watson-Crick base pairing and high target specificity. However, although the ASO concept was first demonstrated as far back as 1978[10], ASOs have only recently started to deliver on their initial promise. Fifteen oligonucleotides have been approved for clinical use (twelve since 2016) indicating their increasing therapeutic value.[11] Until recently all of these were for rare life limiting diseases, but the field just received a major boost with the EMA and NICE approval of the Novartis siRNA drug Inclisiran (Leqvio) for lowering LDL cholesterol levels in patients with hypercholesterolemia[12]. Unlike previous oligonucleotide therapeutics, Inclisiran is used to treat a very common chronic disease. Although a major triumph, and an insight into what the future could hold for oligonucleotide therapeutics, Inclisiran is a special case where targeted delivery to the liver is required. Other organs are more difficult to penetrate, and inefficient biodistribution, poor cellular delivery, and toxicity prevent the wider adoption of antisense technology. Given these limitations, new oligonucleotide analogues are urgently needed to advance the field.

To achieve a therapeutic response an oligonucleotide must be stable *in vivo*, bind to its target RNA with high selectivity and affinity, and display good pharmacokinetic properties[2]. Unmodified oligonucleotides

are rapidly digested by nucleases in cells and are therefore completely unsuitable. Modifications designed to provide nuclease resistance[13] include 2´-OMe, 2´-*O*-(2-methoxyethyl), 2´-fluoro sugars[14-16], and phosphorothioate (PS) backbones (Fig. 1a)[15, 17]. The PS group improves cell uptake but reduces RNA target affinity, which can be restored by the 2´-sugar substituents[2]. Whilst these modifications have led to oligonucleotide therapies[11], limited efficacy, off-target effects and toxicity remain obstacles to wider adoption in the clinic[18]. Poor uptake into cells is particularly troublesome; less than 1% of an administered oligonucleotide typically reaches its target[19]. Reducing the net anionic charge of oligonucleotides by partial or complete replacement of the phosphodiester backbone with neutral linkages would seem to be a viable strategy for increasing cell permeability and nuclease resistance[13, 20]. A clinically relevant example[21] is the phosphorodiamidate morpholino backbone (PMO) (Fig. 1a), but limitations in solid phase syntheses complicate the assembly of charge-reduced PMO–DNA chimeras. Most other uncharged backbones that have been studied reduce the affinity and selectivity of therapeutic oligonucleotides towards their RNA targets[13]. However, we felt that the 'reduced charge' principle warranted detailed investigation. Oligonucleotides containing the artificial amide backbone AM1 (Fig. 1b) are of interest as they form moderately stable duplexes with complementary RNA[22 23-27]. Despite this, the required monomers have not been synthesised for all four canonical nucleobase analogues[28]. Inspired by the extremely high target affinity of locked nucleic acids (LNA) (Fig. 1b) developed in the 1990's[29-32], we hypothesised that conformationally locking the nucleosides surrounding the AM1 linkage would produce reduced-charge oligonucleotides (ONs) with higher target affinity, and in combination with PS linkages might yield ASOs with superior cell uptake and *in vivo* stability. Although attaching LNA sugars directly to other non-phosphorus-based charge-neutral backbones has so far failed to produce analogues with increased duplex stability[33-38] we reasoned that AM1, being a particularly close analogue of the phosphodiester backbone[39], might behave differently (Fig. 1c).

Here, we describe the synthesis of oligonucleotides containing LNA-amide linkages and show that these can be combined with phosphodiester or phosphorotioate backbones. We demonstrate the excellent duplex stabilisation of the LNA-amide linkages, mismatch discrimination and extreme resistance to nucleases. Preliminary studies show that LNA-amide ONs containing PS backbones have improved cellular uptake and are highly effective in exon-skipping assays.

Results And Discussion

LNA-amide monomer synthesis is efficient and scalable

Efficient synthesis of chemically modified oligonucleotides is essential to fuel fundamental studies and therapeutic applications. We have devised a strategy which enables the straightforward assembly of oligonucleotides containing LNA-flanked amides which could be easily automated and scaled up. A

maximum of eight monomers are required to make any sequence that contains non-contiguous amide linkages (four carboxylic acids and four amines).

Attaching the required ethanoic acid moiety to the 3´-carbon of the LNA sugar is challenging as it requires removal of the 3´-oxygen and formation of a C-C bond. However, we were able to produce the required 5´-dimethoxytrityl (DMT)-protected 3´-ethanoic acid LNA-monomers in 8 steps from **1**, the same number as for conventional LNA phosphoramidites[43] (Fig. 2a). Moreover, we did this with minimal chromatography. We first built the sugar with the C3´-ester **5**, before addition of the nucleobase. This approach avoids complications associated with forming a C-C bond at the 3´-side of a nucleoside using the Barton-McCombie reaction[23-25, 44] or the hydrogenation step if a Wittig reaction is used[45, 46], which would ultimately limit the range of heterocyclic bases that can be added. Key intermediate **5** was readily prepared on multiple gram scale in 81% overall yield from commercially available **1** without the need for chromatographic separation as follows. Hydrogenolysis of compound **1** afforded alcohol **2** which was subsequently oxidised to give compound **3**. Olefination of **3** with (carbethoxymethylene)triphenylphosphorane (Wittig reaction) selectively yielded **4** as the (*E*)-stereoisomer (Fig. 2b). Catalytic hydrogenation of **4** using Pd/C and H_2 gave **5** as a single stereoisomer (Fig. 2b). This stereoselectivity was predicted because the 1,2-*O*-isopropylidene groups on the α-face of furanosyl carbohydrate derivatives direct incoming H_2 to the β-face[47]. Key intermediate **5** was then converted to the 1,2-di-*O*-acetate glycosyl donor **6** following a procedure reported by Arzel *et al.*[48], avoiding the formation of a lactone which occurred when the acetonide was cleaved in the presence of water.

The pathways to each monomer then diverged, with Vorbrüggen conditions[43, 49] utilised for addition of the nucleobases to access **7a-e**. Subsequent simultaneous unmasking of the 3´-carboxyl and 2´-hydroxyl groups by treatment with hydroxide, followed by cyclisation to form the 2´- 4´-oxymethylene bridge, then 5´-mesyl deprotection, gave the hydroxy-LNA acid compounds **8a-e**. The progress of the reaction was rapid; mesyl deprotection using hydroxide ion conventionally requires several days under reflux conditions[43]. We postulate that the acceleration in rate is due to neighbouring group participation whereby the carboxylate anion displaces the 5´-mesyl group, forming a lactone that is subsequently opened by hydrolysis (Supplementary Fig. 1). Finally, we treated the resulting hydroxy-acids **8a-e** with 4,4´-dimethoxytrityl chloride (DMT-Cl) in pyridine to give the DMT-protected LNA analogue nucleosides **9a-e**.

Using this strategy we were able to access all four canonical nucleoside analogues along with the 5-methylcytidine monomer which is used in place of cytidine in antisense experiments to increase target affinity and improve other therapeutic properties[18]. Additionally, we required 5´-MMT-amino LNA phosphoramidite **10**. Whilst this had been previously synthesised[40] we chose to develop a more efficient route (Supplementary Fig. 2). Commercially available 5´-MMT-amino dT **11** and 5´-DMT thymidine-3

´-ethanoic acid **12**[41, 42] (Fig. 2c) were also required to enable us to make oligonucleotides to compare the properties of DNA amide with those of LNA-amide.

Chimeric oligonucleotides can be synthesised in high purity

Our oligonucleotide synthesis strategy is shown in Fig. 3. A phosphoramidite monomer with an MMT-protected 5´-amino group, either LNA **10**[40] or deoxythymidyl **11**, is added to the oligonucleotide, and the amine is deprotected using trichloroethanoic acid. An LNA-acid (or DNA-acid[50]) monomer is coupled to the free amine using PyBOP activating agent in the presence of a non-nucleophilic base (*N*-methylmorpholine) to form the amide bond. Oligonucleotide synthesis is then resumed, starting with removal of the DMT group.

The process is repeated to install multiple non-contiguous amides in the same oligonucleotide. To demonstrate this, DMT-protected LNA acids **9a-e**, phosphoramidites **10** and **11**, and DNA acid **12**[41, 42] (Fig. 2), were used to synthesise several oligonucleotides, some of which contain multiple additions of LNA-amide, 2´-OMe sugars and PS linkages (Supplementary Table 1). In all cases, we obtained the oligonucleotides in high purity. High-performance liquid chromatography (HPLC) and mass spectrometry demonstrated the high incorporation efficiency for the DMT-protected LNA acids **9a-e** (Supplementary Fig. 3-7).

LNA sugars stabilise duplexes containing the amide backbone

To evaluate the ability of the LNA-amide combination to bind to complementary RNA with high affinity we synthesised a series of 13-mer ONs with a central amide with a T-T sequence. These constructs were composed of either no LNA (ON1$^{\text{DNA-Am-DNA}}$), an LNA 5´ to the amide (ON2$^{\text{LNA-Am-DNA}}$), an LNA 3´ to the amide (ON3$^{\text{DNA-Am-LNA}}$), or LNA on both sides of the amide (ON4$^{\text{LNA-Am-LNA}}$, Fig. 4a). Controls without amide (ON5$^{\text{LNA-LNA}}$ and ON6$^{\text{DNAcontrol}}$) were also made. We compared duplex denaturation temperatures (T_ms) after hybridisation with DNA and RNA complementary strands (Fig. 4b, Supplementary Table 2, Supplementary Fig. 8 and 9). ON2$^{\text{LNA-Am-DNA}}$ produced a significant increase in DNA:RNA hybrid stability, (+3.0 ˚C) compared to the unmodified ON6$^{\text{DNAcontrol}}$, and an increase of +3.4˚C compared to 'amide only' ON1$^{\text{DNA-Am-DNA}}$. Importantly, ON4$^{\text{LNA-Am-LNA}}$, in which the amide is surrounded by LNA sugars, gave the greatest increase in stability (+5.1 ˚C). It is noteworthy that ON2$^{\text{LNA-Am-DNA}}$ and ON4$^{\text{LNA-Am-LNA}}$ provide the first examples of duplex stabilisation by an LNA sugar attached to a non-phosphorus artificial DNA backbone. The RNA target selectivity of LNA-amide-containing ONs was excellent; a single mismatched base pair greatly reduced duplex stability, in some cases by >14 ˚C (Supplementary Table 2,

Supplementary Fig. 10-13) In summary, an amide linkage flanked by LNA on both sides gives strong DNA:RNA duplex stabilisation and good mismatch discrimination.

In duplexes with DNA targets, ONs with all combinations of LNA and DNA sugars around the amide linkage were slightly destabilising (between -0.1 ˚C to -2.6 ˚C), indicating the selectivity of the amide linkage for complementary RNA. The stabilisation induced by the LNA amide combination is cumulative and general (Fig. 4c, Supplementary Table 3, Supplementary Fig. 14-17). In a biologically relevant sequence context, four LNA-amides increase duplex stability against complementary RNA by an impressive 13.0 ˚C compared to only 5.1 ˚C for the DNA target. This large difference is important when developing oligonucleotides to interact with RNA. Oligonucleotides for *in vivo* studies usually contain 2´-OMe modified sugars and/or phosphorothioate backbones to prevent degradation by nucleases. In such oligonucleotides the combination of LNA and amide also greatly increases duplex stability (Supplementary Table 3).

Combining LNA and amide provides strong nuclease resistance

Therapeutic oligonucleotides must remain stable in cells for prolonged periods to remain active. To evaluate whether the combination of LNA and amide confers greater nuclease resistance than LNA alone, we incubated unmodified DNA ($ON15^{DNA/17PO}$) and DNA with four LNA-amide linkages ($ON14^{DNA/4LAL/13PO}$) in a 1:1 mixture of phosphate buffered saline (PBS) and foetal bovine serum (FBS) to mimic the *in vivo* environment, and compared it to the equivalent construct with LNA but without amide linkages ($ON25^{DNA/8LNA/17PO}$, Supplementary Fig. 18). The results show that the combination of LNA and amide confers extreme resistance to nucleases. Both the oligonucleotides lacking amide linkages had partially degraded within 1 hour whereas $ON14^{DNA/4LAL/13PO}$ remained intact after 8 hours. Interestingly ON14 shows stability at its 3´-end, even though this region has an unmodified sugar phosphate trimer. The 3´-terminal pentamer region, however, is highly modified. It has reduced charge due to the amide linkage and also contains two LNA sugars. It may therefore not be recognised by nucleases. This enhanced stability further illustrates the advantages of removing charge and including modified sugars in antisense oligonucleotides.

X-ray crystallography of the LNA-amide modification

We solved several X-ray structures to determine the effects of LNA and amide modifications on duplex structure and conformation. These are the first crystal structures of DNA:RNA hybrids that contain amide linkages. An amide-modified RNA:RNA duplex was analysed previously, but this had amides in *both* strands surrounded by multiple mismatched base pairs which cannot exist outside the solid-state at ambient temperature[27]. The sequence of the modified DNA:RNA hybrid duplexes (Supplementary Table 4) was based on the corresponding unmodified version (d-CTTTTCTTTG/rCAAAGAAAAG)[51] (the location of

the amide is underlined). Good quality crystals diffracting between 2.5-2.8 Å resolution were obtained for the DNA:RNA hybrid in which the DNA strand contains an amide linkage flanked by DNA on both sides, LNA on both sides and with LNA only on the 5´-side (Supplementary Fig. 19). The unmodified DNA:RNA duplex was also studied. The data collection and refinement statistics are given in Supplementary Table 5. Electron density maps at the modification position for the four nucleic acid crystal structures reported in this manuscript are given in Supplementary Fig. 20.

The hybrids with amide and LNA-amide backbones (Fig. 5a) are structurally very similar to the unmodified duplex (all-atom RMSD 0.4 Å) as shown by their superimposition (Fig. 5a, Supplementary Fig. 21). All structures adopt the A-conformation with sugar puckers clustering around C3´-*endo* (Supplementary Fig. 22). As expected, all duplexes are stabilised by canonical Watson-Crick base pairs, indicating that the thermodynamic improvements due to the LNA-amide backbones are not due to unusual changes in hydrogen bonding interactions. In agreement with the DNA:RNA hybrid NMR structure by Rosners[22] in which the DNA strand contained multiple amides, our X-ray studies indicate that the amide linkage is a close mimic of the phosphodiester backbone (Fig. 5b). Both are four-atom linkages, hence similar in length, and the amide carbonyl is orientated in the same direction as one of the phosphodiester P-O bonds.

In Fig. 5c, the structures of all amide backbones are overlaid to assess the effects of the LNA modifications. Between each structure, the orientation of the backbone is consistent, directing the amide oxygen into the major groove. Other atomic positions of the backbones also show close similarity, and the presence of 3´-LNA causes no significant distortion. 5´-LNA does however cause some structural displacement; the 5´-sugars in the LNA-amide-DNA and LNA-amide-LNA structures are shifted slightly outwards compared to the DNA-amide-DNA and unmodified strands. Despite this, the positioning of the amide backbone remains consistent between each structure. The amide adopts the expected *trans*-conformation, and LNA on the 5´-side of the amide has little effect on backbone torsion angles (Fig. 5c, Supplementary Fig. 23). In summary, combined LNA and amide modifications have minimal effect on the duplex structure, and are excellent mimics of natural phosphodiesters.

Combining LNA-amide and PS enhances gymnotic delivery

In a preliminary study we have evaluated the biological activity of the LNA-amide combination using the HeLa pLuc/705 cell line[52] that carries a luciferase-encoding gene interrupted by a mutated ß-globin intron[52]. This mutation creates a 5´-splice site which activates a cryptic 3´-splice site, resulting in incorrect mRNA splicing and the production of non-functional luciferase. An oligonucleotide that hybridises to the mutant 5´-splice site prevents incorporation of the aberrant intron, restoring the pre-mRNA splicing to produce functional luciferase, which is quantified by luminometry. Oligonucleotides complementary to this aberrant splice site were synthesised with combinations of different modifications to determine their

individual effects (Supplementary Table 3). ON14$^{DNA/4LAL/13PO}$, ON16$^{2¢OMe/4LAL/13PO}$, and ON18$^{2¢OMe/4LAL/13PS}$ were designed to evaluate LNA-amide with the DNA, 2´-OMe/phosphodiester, and 2´-OMe/phosphorothioate backbones respectively, and ONs 14 and 16 were included to determine the degree to which LNA-amide influences delivery, activity and toxicity in the absence of PS linkages. LNA and amide linkages are incompatible with RNase-H so there is no risk of ON14 or ON16 inadvertently destroying the RNA target[2,56]. Three controls were included: ON20$^{2¢OMe/17PS}$ (which represents the gold standard in the assay) to determine whether LNA-amide enhances biological activity[52], ON17$^{2¢OMe/17PO}$ to evaluate the effects of the PS linkage independently of LNA or amide linkages, and ON19$^{2¢OMe/8LNA/17PS}$ with LNA sugars but no amide linkages to determine the effects of the enhanced duplex stability caused by LNA. A scrambled control with a 2´-OMe/PS backbone was also included to determine off target effects (ON31$^{2¢OMe/17PS\ scrambled}$, Fig. 6).

To compare biological activity independent of cell uptake, Lipofectamine 2000 (LF2000), a cationic liposome transfection/delivery reagent, was used. All three target-complementary PS-ONs were active in the assay (ON20$^{2¢OMe/17PS}$, ON18$^{2¢OMe/4LAL/13PS}$, and ON19$^{2¢OMe/8LNA/17PS}$), whereas all the PO-ONs (ON14$^{DNA/4LAL/13PO}$, ON16$^{2¢OMe/4LAL/13PO}$ and ON17$^{2¢OMe/17PO}$) were inactive at 100 nM (Fig. 6a). Hence, in agreement with previous studies, the phosphorothioate modification in a target-complementary sequence is necessary for splice-switching activity. This could result from the PS groups enhancing nuclear enrichment[53] of the oligonucleotides, and/or recruiting ILF2/3 to the RNA transcript[54]. Notably, the addition of the amide linkage significantly improved the splice-switching activity of 2´-OMe/PS ONs at the lower concentrations (6.25 nM and 12.5 nM), probably due to improved target affinity (Fig. 6b).

Next, we compared the naked (gymnotic) uptake of the ONs. These conditions more closely represent *in vivo* applications where transfection agents such as LF2000 cannot be used. We seeded cells at low confluency, added the oligonucleotides in fresh media after 16 h, and measured luciferase activity after a further 96 h. The presence of just four LNA-amides (ON18$^{2¢OMe/4LAL/13PS}$) significantly increased activity in a dose-dependent manner compared to ON20$^{2¢OMe/17PS}$ (Fig. 6c). Greater than 5-fold increase in activity was observed for gymnotic delivery compared to a maximum of 3-fold increase for the LF2000-mediated transfection. This suggests that synergy between the PS and LNA-amide modifications leads to enhanced productive delivery into cells. The improved therapeutic properties of LNA-amide/PS oligonucleotides observed in these preliminary studies are possibly due to a combination of reduced charge from the LNA-amides and interactions of the PS backbone with cellular components. Improved cell uptake may result from the neutral amide linkages breaking up the poly-anionic backbone into short segments which penetrate cells more readily than long poly-anionic stretches. Interestingly, ON19$^{2¢OMe/8LNA/PS}$ with LNA and no amides showed only slight dose response in activity, even at the highest concentration tested (Fig. 6c, Supplementary Fig. 24). This could be due to its binding to off-

targets, altered rigidity, or undesirable secondary structures induced by the extreme stability caused by the LNA sugars, reducing the ability of the ON to interact with the cell surface, a mechanism for productive uptake. ON16$^{2¢OMe/4LAL/13PO}$ with LNA-amides and no PS linkages also displayed slight gymnotic splice-switching activity (Supplementary Fig. 24).

We compared the viability of the HeLa cells following lipofection using a WST-1 cell proliferation assay (Fig. 6d). At the highest concentration tested (400 nM) the cells treated with ON20$^{2¢OMe/17PS}$ were only 21% viable, whereas the cells treated with the same concentration of ON18$^{2¢OMe/4LAL/13PS}$ were 50% viable, demonstrating that the LNA-amide linkage significantly reduces the cytotoxicity of ONs delivered with LF2000. This is verified by analysis of the protein levels (Supplementary Fig. 25) and visible cell death (Fig. 6e, and Supplementary Fig. 26). It supports the use of the combination of LNA-amide, 2´-OMe and PS modifications for *in-vitro* studies. Interestingly, the oligonucleotide containing eight LNA sugars without amide linkages (ON19$^{2¢OMe/8LNA/17PS}$) had a poor toxicity profile. This could be due to off-target effects and could also explain why, despite showing the highest affinity towards RNA in the UV melting studies, the LNA modified ON19$^{2¢OMe/8LNA/17PS}$ was not the most active in the exon-skipping assay. Further detailed studies are required to determine whether this is a general or a sequence specific phenomenon, and to validate its relevance in terms of toxicity.

Given that cell uptake and toxicity remain major challenges when developing new therapeutic oligonucleotides the results in Fig. 6 suggest that our modification strategy could be advantageous. The synergistic effect of LNA-amide linkages and phosphorothioate modifications appear to produce oligonucleotides with enhanced biological properties. However, cell culture studies cannot address some of the major challenges in oligonucleotide therapeutics, particularly those that relate to pharmacokinetics, pharmacodynamics, biodistribution and aspects of toxicity. We are therefore planning further detailed biological studies on LNA-amide-phosphorothioate oligonucleotides to answer these important questions.

Conclusions

We have developed a high yielding methodology to synthesise oligonucleotides containing uncharged LNA-amide linkages. The chemistry has the potential to be automated and carried out at scale for therapeutic oligonucleotide development. These new constructs have high resistance to enzymatic degradation and bind to complementary RNA with affinity and selectivity superior to unmodified ONs. The artificial backbone causes minimal structural deviation in DNA:RNA hybrids, consistent with their strong affinity for RNA. Oligonucleotides with alternating LNA-amide and phosphodiester (or phosphorothioate) backbones cannot give rise to recyclable LNA mononucleotides (modified dNTPs) in the presence of cellular nucleases, and their favourable toxicity profile relative to LNA in these initial studies may reflect this. In studies with gymnotic (naked) delivery, combining LNA-amides with phosphorothioates improves cell uptake. Poor cellular uptake is currently a major barrier in oligonucleotide therapeutics and combining the PS and LNA modifications with charge-neutral amide backbones such as AM1 could lead to improved

clinical efficacy. Research is in progress to explore these new analogues in a range of cellular assays and in other therapeutic interventions such as siRNA and RNase-H mediated antisense inhibition.

Finally, artificial nucleic backbones are of interest to researchers in many other fields including nucleic acid chemistry, chemical biology, biochemistry, medicinal chemistry, diagnostics, gene synthesis, gene editing, nanotechnology, materials chemistry and biophysics. We hope that this work will catalyse future research in these areas.

Methods

Amide-modified oligonucleotide synthesis

Oligonucleotide segment synthesis. Oligonucleotide synthesis was performed on an Applied Biosystems 394 automated DNA/RNA synthesiser on a 1.0 μmole scale using a standard phosphoramidite cycle of detritylation, coupling, and oxidation. No capping step was used. All β-cyanoethyl phosphoramidite monomers were dissolved in anhydrous MeCN (10% CH_2Cl_2 was added when 2'-OMe U phosphoramidite was used) to a concentration of 0.1 M immediately prior to use. 5-(Benzylthio)-1*H*-tetrazole (BTT) activator (0.3 M) was used with a coupling time of 50 s for normal dA, dG, dC and T phosphoramidites, this was extended to 6 min for 2'-OMe and LNA phosphoramidites. Standard iodine oxidiser was used for phosphodiester oligonucleotides. For the phosphorothioate oligonucleotides, 3-ethoxy-1,2,4-dithiazoline-5-one (EDITH) was used as the sulfurisation agent, and the solid support was washed with MeCN after each phosphoramidite coupling before the sulfurisation step. Sulfurisation time was initially 3 min, and after this period fresh EDITH was sent to the synthesis column and left for another 3 min. Further details are given in the Supplementary Information.

Amino monomer addition. The MMT-protected 5´-amino phosphoramidite monomer (either LNA **10**[40] or commercially available deoxythymidyl **11**) was dissolved in anhydrous MeCN to a concentration of 0.1 M immediately prior to use. The same coupling conditions as above were used, but the coupling time was extended to 10 min. The MMT protecting group was cleaved on the Applied Biosystems 394 automated synthesiser using 3% TCA in CH_2Cl_2 with an extended cleavage time of 2 min. The solid support was then washed with acetonitrile on the synthesiser for 3 min. To improve the coupling efficiency in the next step, the solid support was washed with 0.5% (v/v) *N*-methylmorpholine in DMF (1 x 1mL) followed by DMF (3 x 1 mL).

Amide bond formation on resin (peptide coupling). All amide couplings were performed manually on the synthesis column. A solution with 10 equivalents of acid monomer, 10 equivalents of PyBOP and 30 equivalents of *N*-methylmorpholine was first prepared in 400 μL of DMF. This was then taken up into a 1 mL syringe and loaded onto the column before a second 1 mL syringe was attached to the other end of the synthesis column. The mixture was agitated every 10 min for 1 h. The columns were then washed with DMF (3 x 1 mL) followed by MeCN (5 x 1 mL) and dried by passing argon through the column. The column was then returned to the synthesiser to continue oligonucleotide synthesis.

Cleavage of oligonucleotides from resin, deprotection and purification. LNA-amide containing oligonucleotides were isolated with the final 5'-DMT protecting group still in place (DMT-ON). Following solid phase synthesis, the cyanoethyl groups were removed by a 15 min treatment with 20% diethylamine in MeCN. The resin was then washed with MeCN (5 x 1 mL) and dried by passing a stream of argon through the synthesis column. The oligonucleotides were cleaved from the solid support and deprotected by heating in concentrated aqueous ammonia in a sealed glass vial at 55 °C for 5 hours. The ammonia was removed under reduced pressure prior to oligonucleotide purification. The DMT-ON oligonucleotides were purified by reverse-phase high performance liquid chromatography (RP-HPLC) and lyophilised. They were then dissolved in 0.5 mL of 80% acetic acid and left for 1 hour at room temperature to remove the DMT group. The solution was neutralised with 0.5 mL of triethylammonium acetate buffer (2 M, pH 7) and the detritylated oligonucleotides were desalted using a NAP-10 column (Cytiva) then freeze dried.

Data availability

Crystallographic data for the structures in this Article have been deposited at the Cambridge Crystallographic Data Centre under deposition numbers CCDC 2105684 and 2105685.DNA structural data obtained by X-ray crystallography were deposited in the Protein Data Bank (PDB) and are available with the following accession codes 7NRP, 7OOS, 7OZZ and 7OOO. Source data is provided for Fig. 6 and Supplementary Figs. 24 and 25. The authors declare that all other data supporting the findings of this study are available within the paper and its supplementary information files.

Declarations

Acknowledgements

The authors would like to thank Dr Samir El-Andaloussi for the HeLa pLuc/705 cell line[52]. This work was funded in part by a BBSRC research grant to TB (New oligonucleotide analogues for therapeutic applications. BB/S018794/1).

Author contributions

Y.R.B, L.M.P, L.L and P.K performed the small molecule synthesis; Y.R.B, L.M.P and K.E.C carried out the small molecule crystallography work; Y.R.B, A.E.S, J.C, S.E and D.S synthesised and purified the ONs; Y.R.B, J.C and L.C performed UV melting and enzymatic stability studies; C.T, M.A.McD, J.S.H and J.P.H carried out the ON XRD studies; Y.R.B, W.F.L and G.McC performed the cell studies; Y.R.B, A.E.S, P.K and T.B. designed the study. All authors contributed to the writing of the manuscript. T.B. oversaw and managed the project. M.J.A.W oversaw the biological work.

Competing interests

T.B.is a consultant to ATDBio Ltd.

References

1. Smith, C.I.E. & Zain, R. Therapeutic Oligonucleotides: State of the Art. Annu. Rev. Pharmacol. Toxicol. **59**, 605–630 (2019).
2. Khvorova, A. & Watts, J.K. The chemical evolution of oligonucleotide therapies of clinical utility. Nat. Biotechnol. **35**, 238–248 (2017).
3. Rinaldi, C. & Wood, M.J.A. Antisense oligonucleotides: the next frontier for treatment of neurological disorders. Nature Reviews Neurology **14**, 9–21 (2018).
4. Liang, X.-H., Sun, H., Nichols, J.G. & Crooke, S.T. RNase H1-Dependent Antisense Oligonucleotides Are Robustly Active in Directing RNA Cleavage in Both the Cytoplasm and the Nucleus. Mol. Ther. **25**, 2075–2092 (2017).
5. Dominski, Z. & Kole, R. Restoration of correct splicing in thalassemic pre-mRNA by antisense oligonucleotides. *Proc. Natl. Acad. Sci. U. S. A.* **90**, 8673–8677 (1993).
6. Sierakowska, H., Sambade, M.J., Agrawal, S. & Kole, R. Repair of thalassemic human beta-globin mRNA in mammalian cells by antisense oligonucleotides. *Proc. Natl. Acad. Sci. U. S. A.* **93**, 12840–12844 (1996).
7. Aartsma-Rus, A. et al. Therapeutic antisense-induced exon skipping in cultured muscle cells from six different DMD patients. Hum. Mol. Genet. **12**, 907–914 (2003).
8. Setten, R.L., Rossi, J.J. & Han, S.-p. The current state and future directions of RNAi-based therapeutics. Nature Reviews Drug Discovery **18**, 421–446 (2019).
9. Warner, K.D., Hajdin, C.E. & Weeks, K.M. Principles for targeting RNA with drug-like small molecules. Nature Reviews Drug Discovery **17**, 547–558 (2018).
10. Zamecnik, P.C. & Stephenson, M.L. Inhibition of Rous sarcoma virus replication and cell transformation by a specific oligodeoxynucleotide. *Proc. Natl. Acad. Sci. U. S. A.* **75**, 280–284 (1978).
11. Xiong, H., Veedu, R.N. & Diermeier, S.D. Recent Advances in Oligonucleotide Therapeutics in Oncology. Int. J. Mol. Sci. **22**, 3295 (2021).
12. Fitzgerald, K. et al. A Highly Durable RNAi Therapeutic Inhibitor of PCSK9. N. Engl. J. Med. **376**, 41–51 (2016).
13. Freier, S.M. & Altmann, K.-H. The ups and downs of nucleic acid duplex stability: Structure-stability studies on chemically-modified DNA:RNA duplexes. Nucleic Acids Res. **25**, 4429–4443 (1997).
14. Cummins, L.L. et al. Characterization of fully 2'-modified oligoribonucleotide hetero- and homoduplex hybridization and nuclease sensitivity. Nucleic Acids Res. **23**, 2019–2024 (1995).
15. Monia, B.P., Johnston, J.F., Sasmor, H. & Cummins, L.L. Nuclease resistance and antisense activity of modified oligonucleotides targeted to Ha-ras. J. Biol. Chem. **271**, 14533–14540 (1996).

16. Martin, P. A New Access to 2'-O-Alkylated Ribonucleosides and Properties of 2'-O-Alkylated Oligoribonucleotides. Helv. Chim. Acta **78**, 486–504 (1995).
17. Eckstein, F. Phosphorothioates, essential components of therapeutic oligonucleotides. Nucleic Acid Ther. **24**, 374–387 (2014).
18. Roberts, T.C., Langer, R. & Wood, M.J.A. Advances in oligonucleotide drug delivery. Nature Reviews Drug Discovery **19**, 673–694 (2020).
19. Godfrey, C. et al. Delivery is key: lessons learnt from developing splice-switching antisense therapies. EMBO Mol. Med. **9**, 545–557 (2017).
20. Meade, B.R. et al. Efficient delivery of RNAi prodrugs containing reversible charge-neutralizing phosphotriester backbone modifications. Nat. Biotechnol. **32**, 1256–1261 (2014).
21. Aartsma-Rus, A. & Krieg, A.M. FDA Approves Eteplirsen for Duchenne Muscular Dystrophy: The Next Chapter in the Eteplirsen Saga. Nucleic Acid Ther. **27**, 1–3 (2016).
22. Selvam, C., Thomas, S., Abbott, J., Kennedy, S.D. & Rozners, E. Amides as Excellent Mimics of Phosphate Linkages in RNA. Angew. Chem. Int. Ed. **50**, 2068–2070 (2011).
23. Idziak, I., Just, G., Damha, M.J. & Giannaris, P.A. Synthesis and hybridization properties of amide-linked thymidine dimers incorporated into oligodeoxynucleotides. Tetrahedron Lett. **34**, 5417–5420 (1993).
24. Lebreton, J., Waldner, A., Lesueur, C. & De Mesmaeker, A. Antisense Oligonucleotides with Alternating Phosphodiester-"Amide-3" Linkages. *Synlett* 1994, 137–140 (1994).
25. De Mesmaeker, A. et al. Amides as a New Type of Backbone Modification in Oligonucleotides. Angew. Chem. Int. Ed. **33**, 226–229 (1994).
26. Hardcastle, T. et al. A Single Amide Linkage in the Passenger Strand Suppresses Its Activity and Enhances Guide Strand Targeting of siRNAs. ACS Chem. Biol. **13**, 533–536 (2018).
27. Mutisya, D. et al. Amide linkages mimic phosphates in RNA interactions with proteins and are well tolerated in the guide strand of short interfering RNAs. Nucleic Acids Res. **45**, 8142–8155 (2017).
28. Kotikam, V. & Rozners, E. Amide-Modified RNA: Using Protein Backbone to Modulate Function of Short Interfering RNAs. Acc. Chem. Res. **53**, 1782–1790 (2020).
29. Hagedorn, P.H. et al. Locked nucleic acid: modality, diversity, and drug discovery. Drug Discovery Today **23**, 101–114 (2018).
30. Singh, S.K., A. Koshkin, A., Wengel, J. & Nielsen, P. LNA (locked nucleic acids): synthesis and high-affinity nucleic acid recognition. Chem. Commun., 455–456 (1998).
31. Singh, S.K. & Wengel, J. Universality of LNA-mediated high-affinity nucleic acid recognition. Chem. Commun., 1247–1248 (1998).
32. Bondensgaard, K. et al. Structural Studies of LNA:RNA Duplexes by NMR: Conformations and Implications for RNase H Activity. Chem. Eur. J. **6**, 2687–2695 (2000).
33. Sharma, V.K. et al. Synthesis and biological properties of triazole-linked locked nucleic acid. Chem. Commun. **53**, 8906–8909 (2017).

34. Kumar, P., Truong, L., Baker, Y.R., El-Sagheer, A.H. & Brown, T. Synthesis, Affinity for Complementary RNA and DNA, and Enzymatic Stability of Triazole-Linked Locked Nucleic Acids (t-LNAs). ACS Omega **3**, 6976–6987 (2018).
35. Kumar, P., El-Sagheer, A.H., Truong, L. & Brown, T. Locked nucleic acid (LNA) enhances binding affinity of triazole-linked DNA towards RNA. Chem. Commun. **53**, 8910–8913 (2017).
36. Thorpe, C., Epple, S., Woods, B., El-Sagheer, A.H. & Brown, T. Synthesis and biophysical properties of carbamate-locked nucleic acid (LNA) oligonucleotides with potential antisense applications. Org. Biomol. Chem. **17**, 5341–5348 (2019).
37. Lauritsen, A. & Wengel, J. Oligodeoxynucleotides containing amide-linked LNA-type dinucleotides: synthesis and high-affinity nucleic acid hybridization. Chem. Commun., 530–531 (2002).
38. Seth, P.P. & Swayze, E.E. Oligomeric compounds comprising neutrally linked terminal bicyclic nucleosides PCT/US2009/039438 ISIS Pharmaceuticals WO/2009/124238 2009
39. Shivalingam, A., Tyburn, A.E.S., El-Sagheer, A.H. & Brown, T. Molecular Requirements of High-Fidelity Replication-Competent DNA Backbones for Orthogonal Chemical Ligation. J. Am. Chem. Soc. **139**, 1575–1583 (2017).
40. Obika, S., Nakagawa, O., Hiroto, A., Hari, Y. & Imanishi, T. Synthesis and properties of a novel bridged nucleic acid with a P3' → N5' phosphoramidate linkage, 5'-amino-2',4'-BNA. Chem. Commun., 2202–2203 (2003).
41. Stork, G., Zhang, C., Gryaznov, S. & Schultz, R. Modified ollgonucleotides. Effect of 4 vs 5-atom chimeric internucleoside linkages on duplex stability. Tetrahedron Lett. **36**, 6387–6390 (1995).
42. Ammenn, J., Altmann, K.-H. & Belluš, D. Aza-Claisen Rearrangement: Synthesis of 5'-branched 5'-aminothymidines. Helv. Chim. Acta **80**, 1589–1606 (1997).
43. Koshkin, A.A., Fensholdt, J., Pfundheller, H.M. & Lomholt, C. A Simplified and Efficient Route to 2'-O, 4'-C-Methylene-Linked Bicyclic Ribonucleosides (Locked Nucleic Acid). J. Org. Chem. **66**, 8504–8512 (2001).
44. Lebreton, J., Waldner, A., Fritsch, V., Wolf, R.M. & De Mesmaeker, A. Comparison of two amides as backbone replacement of the phosphodiester linkage in oligodeoxynucleotides. Tetrahedron Lett. **35**, 5225–5228 (1994).
45. Peterson, M.A. et al. Amide-Linked Ribonucleoside Dimers Derived from 5'-Amino-5'-deoxy- and 3'-(Carboxymethyl)-3'-deoxynucleoside Precursors(1). J. Org. Chem. **64**, 8183–8192 (1999).
46. Kotikam, V. & Rozners, E. Concurrent Hydrogenation of Three Functional Groups Enables Synthesis of C3'-Homologated Nucleoside Amino Acids. Org. Lett. **19**, 4122–4125 (2017).
47. Albrecht, H., Jones, G. & Moffatt, J. 3'-Deoxy-3'-(dihydroxyphosphinylmethyl)nucleosides. Isophosphonate Analogs of Nucleoside 3'-Phosphates. J. Amer. Chem. Soc. **92**, 5511–5513 (1970).
48. Arzel, L. et al. Synthesis of Ribonucleosidic Dimers with an Amide Linkage from d-Xylose. J. Org. Chem. **81**, 10742–10758 (2016).

49. Vorbrüggen, H. Some recent trends and progress in nucleoside synthesis. Acta Biochim. Pol. **43**, 25–36 (1996).
50. Brandsen, B.M., Hesser, A.R., Castner, M.A., Chandra, M. & Silverman, S.K. DNA-Catalyzed Hydrolysis of Esters and Aromatic Amides. J. Amer. Chem. Soc. **135**, 16014–16017 (2013).
51. Kopka, M.L., Lavelle, L., Han, G.W., Ng, H.-L. & Dickerson, R.E. An Unusual Sugar Conformation in the Structure of an RNA/DNA Decamer of the Polypurine Tract May Affect Recognition by RNase H. J. Mol. Biol. **334**, 653–665 (2003).
52. Kang, S.-H., Cho, M.-J. & Kole, R. Up-Regulation of Luciferase Gene Expression with Antisense Oligonucleotides: Implications and Applications in Functional Assay Development. Biochemistry **37**, 6235–6239 (1998).
53. Bailey, J.K., Shen, W., Liang, X.-H. & Crooke, S.T. Nucleic acid binding proteins affect the subcellular distribution of phosphorothioate antisense oligonucleotides. Nucleic Acids Res. **45**, 10649–10671 (2017).
54. Rigo, F. et al. Synthetic oligonucleotides recruit ILF2/3 to RNA transcripts to modulate splicing. Nat. Chem. Biol. **8**, 555–561 (2012).

Figures

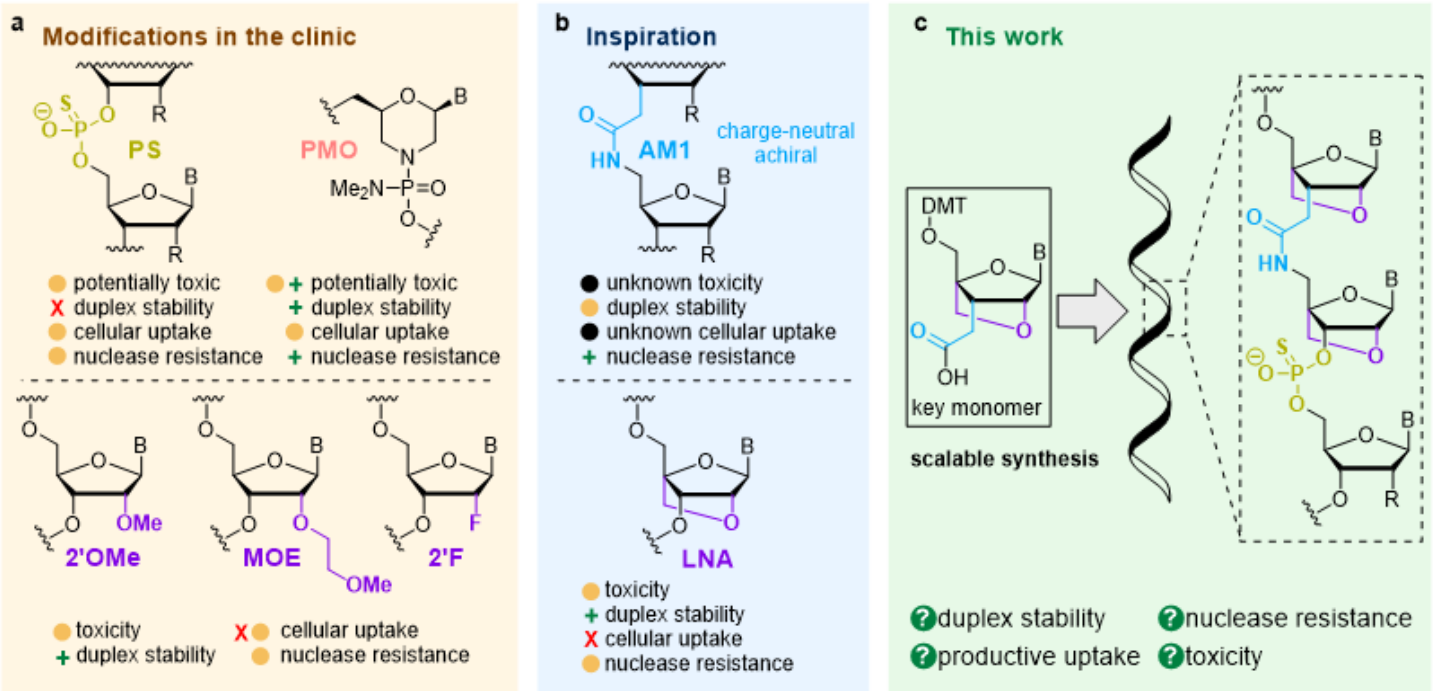

Figure 1

Therapeutic oligonucleotide modifications and our strategy for combining these. ***a.*** *Existing therapeutic oligonucleotide modifications and their properties. Traffic light coding system: green plus = good; amber circle = intermediate; red cross = poor.* ***b.*** *Oligonucleotide modifications that have not yet reached the*

clinic ***c****. Development of a new antisense backbone chemistry with improved target affinity and cellular activity. The LNA-amide linkage is achiral, and can be prepared by solid phase synthesis methods that are high yielding with potential to be automated.*

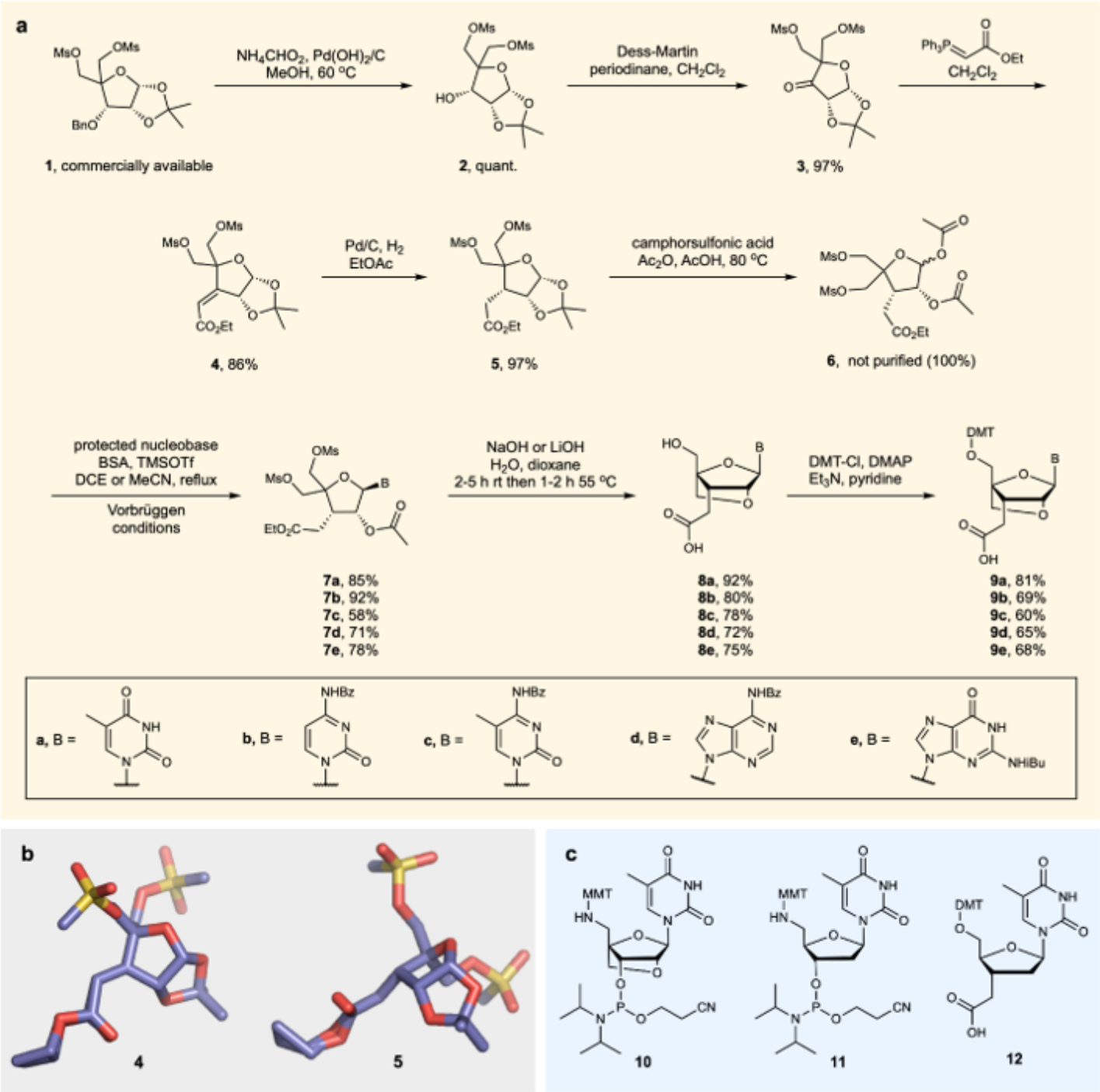

Figure 2

LNA-ethanoic acids and other monomers used in this study. **a.** Synthesis of the DMT-protected LNA ethanoic acids **9a-e**. **b**. X-ray crystal structures confirming the (E)-configuration in **4** and the stereochemistry at the 3´-carbon in **5** (details in the Supplementary Information). **c**. Phosphoramidites

10[40] and **11** (commercially available) and DNA-ethanoic acid monomer **12**[41, 42] used to synthesise oligonucleotides.

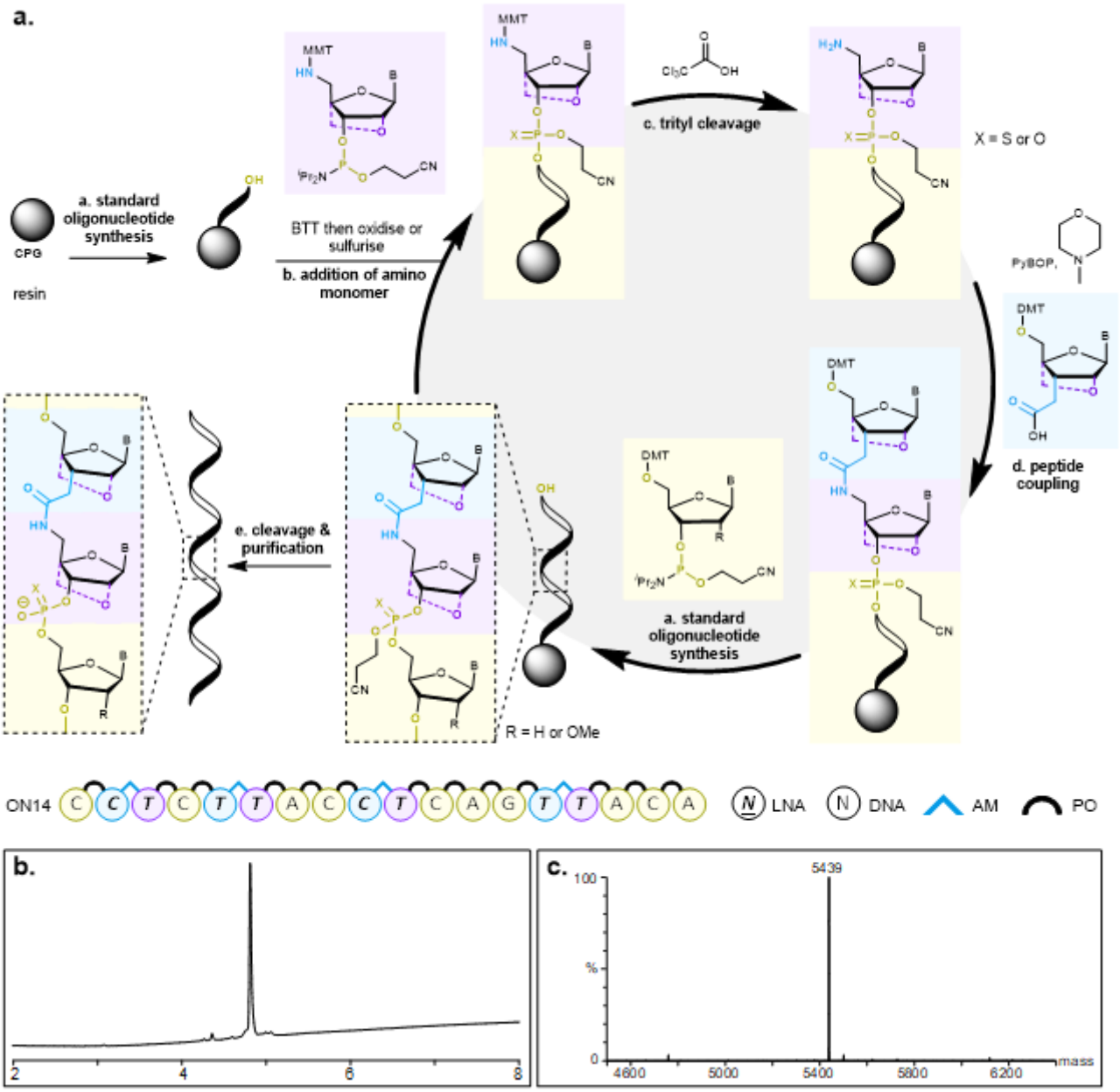

Figure 3

a. *Efficient solid-phase synthesis of amide-phosphodiester chimeras. Dashed lines indicate presence or absence of 2´-4´-methylene bridge. PyBOP = (benzotriazol-1-yloxytripyrrolidinophosphonium hexafluorophosphate.* ***b.*** *Reversed-phase HPLC chromatogram and* ***c.*** *Electrospray (ES-) mass spectrum of a crude LNA-amide chimeric oligonucleotide (ON14). (required mass = 5438.7, found mass = 5439.0).*

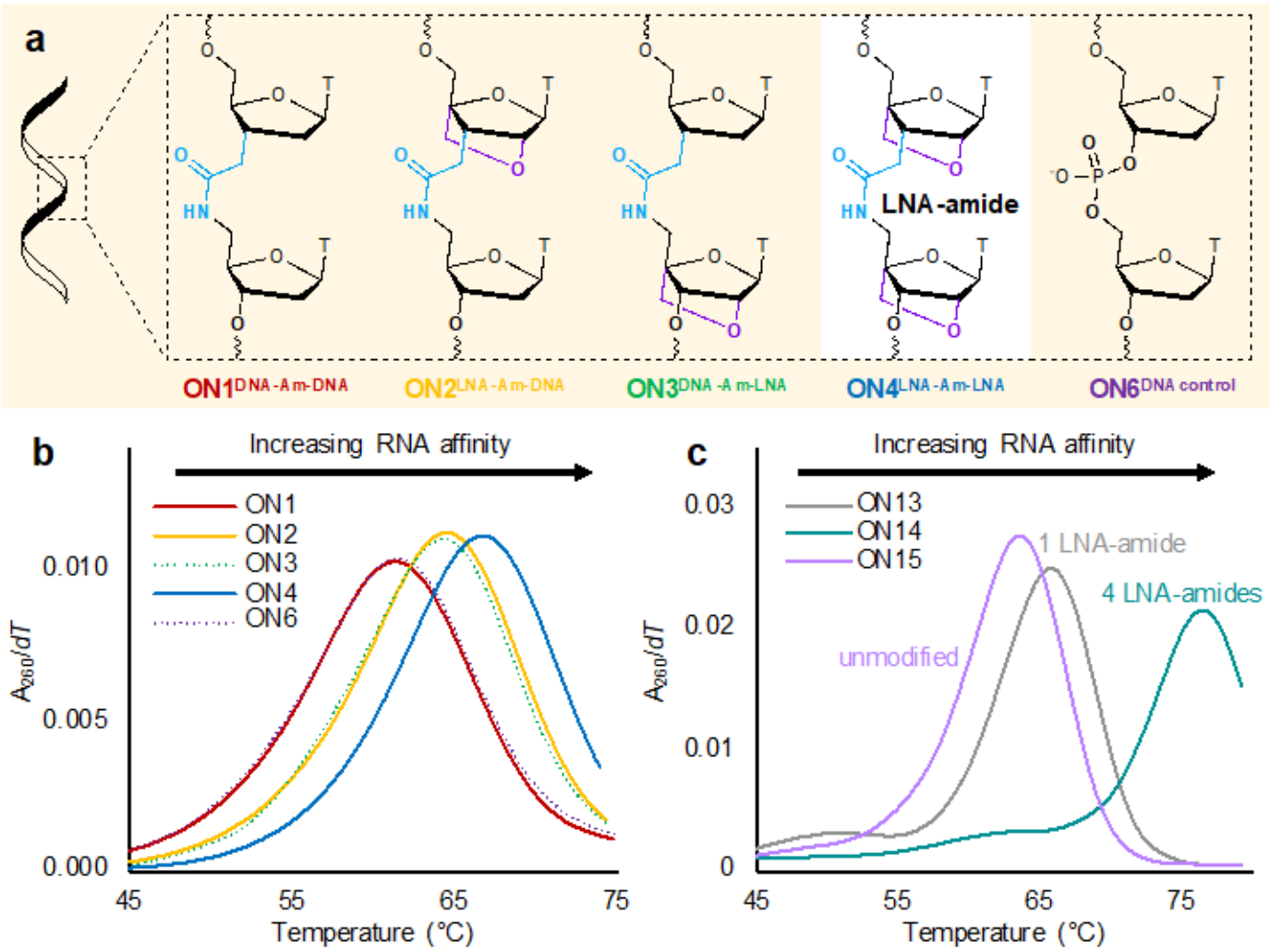

Figure 4

Combining LNA and AM1 increases affinity for complementary RNA. ***a.*** *The structures of each of the LNA AM1 combinations studied. Sequence d-CGACGC**TT**GCAGC (where the underlined region indicates the modification position)* ***b.*** *UV-melting curve derivatives of the ONs from panel* ***a*** *in duplexes with complementary RNA.* ***c.*** *UV-melting curve derivatives demonstrating that the stabilisation conferred by the LNA-amide linkage against complementary RNA is general and cumulative. Conditions: 10 mM phosphate buffer, 200 mM NaCl, pH 7.0. Sequences in Supplementary Table 1.*

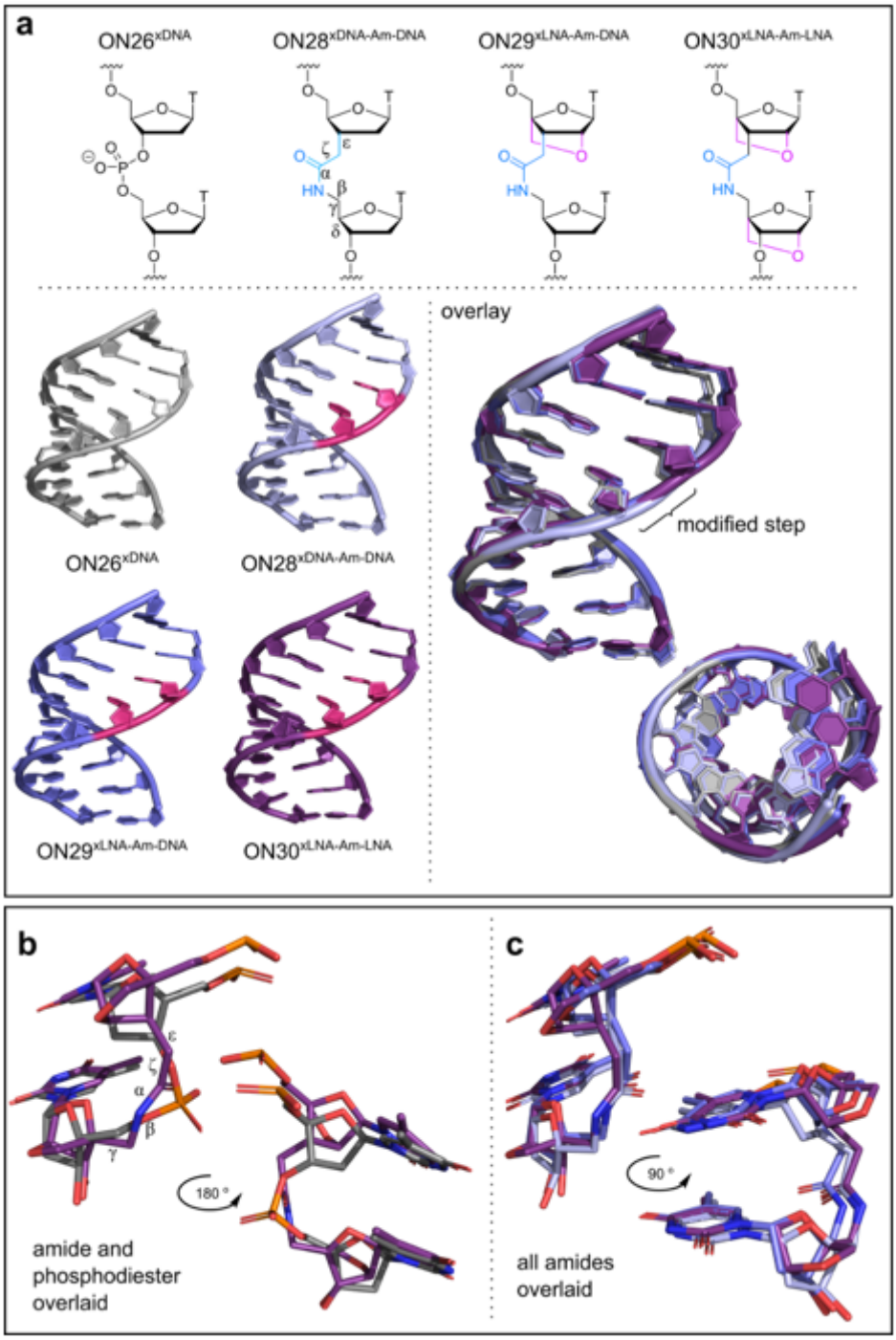

Figure 5

X-ray structures of amide and LNA-amide modified DNA:RNA duplexes. **a**. Structural identity of amide and LNA-amide modifications and the torsion angles of the amide backbone (5´ε → 3´δ). Pink steps show the modification position (left) and the overlay of all structure shows clear similarities (right). **b**. Backbone overlay comparing the LNA-amide-LNA step in ON30$^{xLNA\text{-}Am\text{-}LNA}$ (purple) with the phosphodiester in ON26^{xDNA} (grey). **c**. Overlay of all amide backbones with or without LNA modifications (light blue = ON28$^{xDNA\text{-}Am\text{-}DNA}$, dark blue = ON29$^{xLNA\text{-}Am\text{-}DNA}$, purple = ON30$^{xLNA\text{-}Am\text{-}LNA}$).

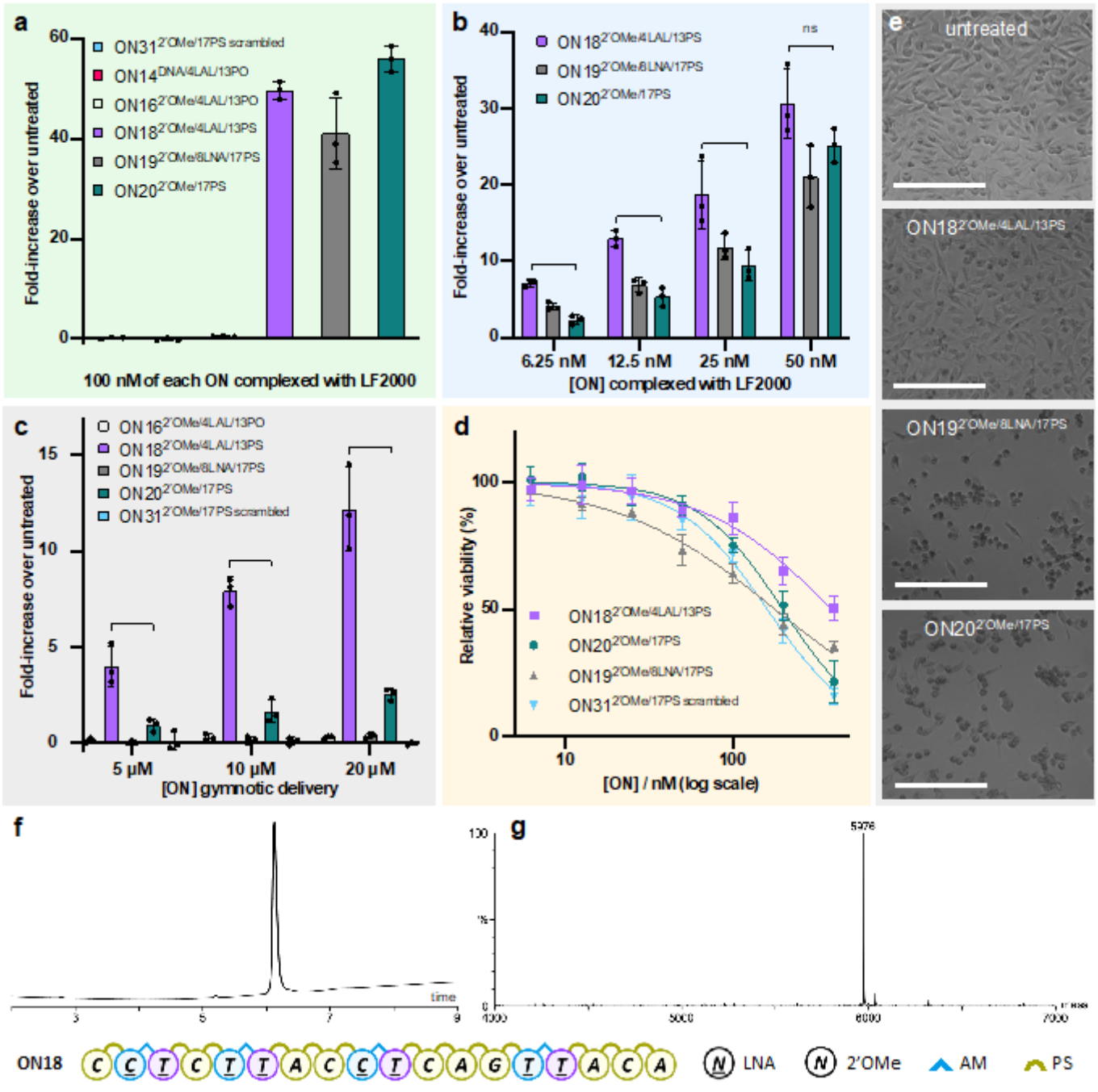

Figure 6

LNA-flanked amides and PS linkages increase gymnotic delivery, exon-skipping activity and reduce toxicity. In all cases luciferase activity was measured and normalised to both protein quantity and untreated cells. Experimental details and sequences are given in the Supplementary Information. ***a.*** *HeLa pLuc/705 cells were transfected at 100 nM ON using LF2000.* ***b.*** *Dose response for active ONs in* ***a****.* ***c.*** *Cells were treated with ONs without transfection agent.* ***d.*** *Viability of the HeLa pLuc/705 cells following lipofection with ONs using LF2000 determined using WST-1 assay.* ***e.*** *Change in cell viability after treatment with 200 nM ONs complexed with LF2000 compared to untreated, scale bar = 200 mm. For all graphs (****a-d****) Data are means ± SD and values for ON18$^{2¢OMe/4LAL/13PS}$ and ON20$^{2¢OMe/17PS}$ were*

*compared by t test analysis. ns represents P > 0.05, * represents P < 0.05, ** represents P < 0.01, *** represents P < 0.001. Each dot represents one distinct replicate (n = 3). ON31$^{2¢OMe/17PS\ scrambled}$: CCUCAUUCACUCGAUUCA.* ***f.*** *Reversed-phase HPLC chromatogram and* ***g.*** *Electrospray (ES-) mass spectrum of purified ON18 used in the assays (required mass = 5976.2, found mass = 5975.5).*

Supplementary Files

This is a list of supplementary files associated with this preprint. Click to download.

- Sourcedata.xlsx
- supportinginformationforNatCommunrevised.pdf
- RS.pdf
- Onlinefloatimage1.png